

Full Paper

New 2-Aryl-1,4-naphthoquinone-1-oxime Methyl Ether Compound Induces Microtubule Depolymerization and Subsequent Apoptosis

Hiromi Sato^{1,*}, Ryota Yamada¹, Midori Yanagihara¹, Hiroko Okuzawa¹, Hiroki Iwata¹, Ayako Kurosawa², Saki Ichinomiya¹, Rina Suzuki¹, Hiroyuki Okabe¹, Tomohiro Yano³, Takuya Kumamoto⁴, Noriyuki Suzuki², Tsutomu Ishikawa², and Koichi Ueno¹

¹Department of Geriatric Pharmacology and Therapeutics, ²Department of Medicinal Organic Chemistry, Graduate School of Pharmaceutical Sciences, Chiba University, 1-8-1 Inohana, Chuoh-ku, Chiba-shi, Chiba 260-8675, Japan

³Department of Life Environmental Sciences, Faculty of Life Sciences, Toyo University, 1-1-1 Izumino, Itakura-machi, Ora-gun, Gunma 374-0193, Japan

⁴Faculty of Pharmaceutical Sciences, Musashino University, 1-1-20 Shin-machi, Nishitokyo-shi, Tokyo 202-8585, Japan

Received December 5, 2011; Accepted January 31, 2012

Abstract. In this study, we describe the antitumor activity of QO-1, one of the new 2-aryl-1,4-naphthoquinone-1-oxime methyl ether derivatives. QO-1 is a derivative of macarpine, a natural occurring product from *Rutaceae* plant. It could potentially inhibit cell growth when tested on 19 cancer cell lines. To investigate its mechanism, two cell lines (HeLa and MCF-7) sensitive to QO-1 were selected. Based on flow cytometry, it was found to induce G₂/M-phase arrest. Moreover, it could cause microtubule depolymerization both in vitro and in vivo. On the other hand, QO-1 activated spindle assembly checkpoint (SAC) proteins. Expression of Bub1, one of the SAC, was gradually increased, reaching a peak after 16 – 20 h, and then gradually decreased. Instead, QO-1 increased the sub-G₁ population, which suggested a cell death population. Actually, expression of Bcl-2 family proteins and activation of caspase-3/7 were evidences of apoptosis. Consistent with these results, cells with DNA fragmentation and multinucleated cells were increased time-dependently after QO-1 exposure. In conclusion, QO-1 has promising antitumor effects via microtubule depolymerization.

Keywords: naphthoquinone-1-oxime, microtubule depolymerization, cytotoxicity, spindle assembly checkpoint, cell cycle

Introduction

Screening for the discovery of potential antitumor active seed compounds from natural sources is still important today. Macarpine, an antitumor-active O₆-benzo[*c*]phenanthridine alkaloid, is one of the attractive compounds. The synthetic pathway of macarpine was established by Ishikawa et al. (1). Additionally they found that one of the key synthetic precursor of macarpine, 6-(6-methoxybenzo[1,3]dioxol-5-yl)naphtho[2,3-*d*][1,3]dioxole-5,8-dione 5-(*O*-methyloxime) (abbreviated QO-1), also showed strong cytotoxic activity (< 0.1 μM)

against the HeLa S3 cell line. QO-1 is one of the 2-aryl-1,4-naphthoquinone-1-oxime methyl ether derivatives. The chemical name and structure of QO-1 along with those of macarpine are shown in Fig. 1A. It has been suggested in a preliminary experiment on the structure–activity relationship (SAR) that the 6,7-methylenedioxy-1,4-naphthoquinone-1-oxime methyl ether skeleton, a common core structure in the 2-aryl-1,4-naphthoquinone-1-oxime methyl ether derivatives, could play an important role for the activity of these compounds (2, 3).

As a target of drug development for cancer therapy, microtubules are an effective target for seed compounds of antitumor drugs derived from natural products. There are examples of successful cancer drugs that target microtubules, and to date, microtubules may be considered one of the most validated therapeutic targets identified

*Corresponding author. hiromi-s@chiba-u.jp

Published online in J-STAGE on March 14, 2012 (in advance)

doi: 10.1254/jphs.11229FP

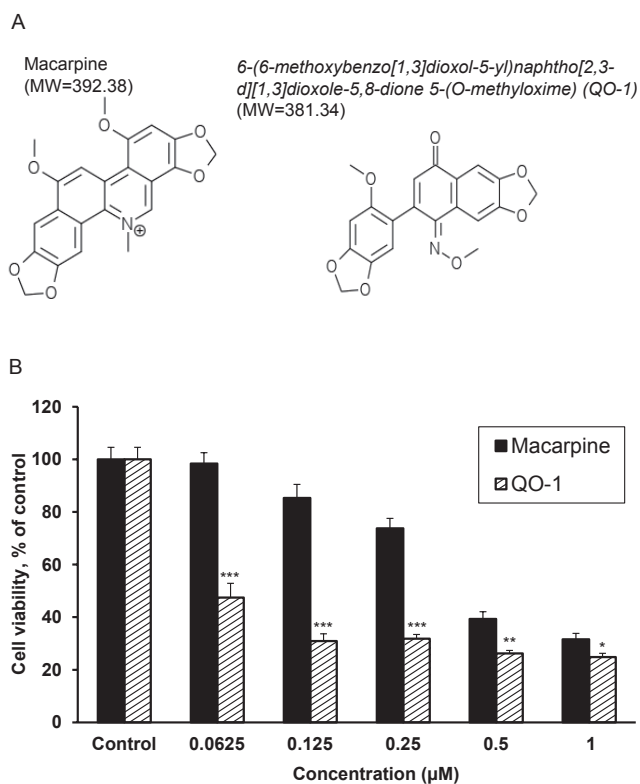


Fig. 1. Growth inhibiting effect of macarpine and QO-1. A: Chemical structures of macarpine and QO-1. Chemical name of QO-1 is 6-(6-methoxybenzo[1,3]dioxol-5-yl)naphtho[2,3-d][1,3]dioxole-5,8-dione 5-(O-methyloxime). B: Effect of macarpine or QO-1 on MCF-7 cell growth. MCF-7 cells were seeded in 96-well plates and treated for 48 h with each compound. Cell viability was evaluated by the MTT assay as described in Materials and Methods. Data shown are each the mean \pm S.D. of three independent experiments. * $P < 0.05$, ** $P < 0.01$, *** $P < 0.001$, compared to macarpine at each concentration (Student's *t*-test).

for cancer therapy. For example, vinblastine, discovered in 1958, is used to treat Hodgkin lymphoma (4), and paclitaxel, isolated in 1971, is used to treat breast cancer and non-small-cell lung cancer (5). These drugs induce apoptosis by damaging DNA, which is recognized at the G₁ checkpoint or by directly attacking microtubules during the M phase (mitotic catastrophe). These drugs are very useful in cancer therapy but can cause serious side effects such as myelosuppression. Additionally, the basic skeletons of these drugs can cause physical problems in drug formulation and limit selection of therapies. However, epothilone, a new tubulin-binding agent, is reported to have a different basic skeleton than existing drugs and fewer side effects (6). Moreover, the novel microtubule inhibitor eribulin (E7389) was approved in April 2011 for the treatment of inoperable recurrent breast cancer. It is a synthetic analog of the marine product halicondrin B. It caused significant and clinically meaningful improve-

ment in overall survival compared with the treatment of physician's choice (7). Therefore, it is important to search for new seed compounds with potent pharmacological activity, especially those stronger than the existing drugs, to improve cancer therapy.

Tubulin-binding agents specifically induce mitotic arrest. In the cell cycle, regulation of the progression from G₂ to M phase is controlled by a cyclin B1-tyrosine dephosphorylated Cdk1 (Cdc2) complex, which modifies cyclin B1 by ubiquitination. This regulation occurs via the spindle assembly checkpoint (SAC) and causes cytotoxicity by induction of apoptosis. Heretofore, an assumption has been made about the mechanism of SAC regulation by tubulin-binding agents (8–10). SAC proteins, including Bub1, Bub3, BubR1, and Mad2, monitor the machinery for attachment of tubulins to kinetochores of chromosomes. This functional system allows normal chromosome separation by inhibition of APC/C, an E3 ubiquitin ligase, and separin, a known as a trigger of anaphase in metaphase (11). For example, Bub1 suppresses the activity of APC/C via phosphorylation of p55Cdc, which is a coenzyme of APC/C (12), and Mad2 directly captures p55Cdc to inhibit the activation of APC/C (13–15).

Compromised or defective function of SAC was discovered in cancer cells almost 100 years ago (16). Chromosomal instability (CIN), which is observed in many cancer cells, leads to an abnormal chromosomal number (aneuploidy) (17) and aneuploidy might promote tumorigenesis and might increase resistance to cancer therapies (18). Diminished expression or activation of SAC proteins tend to induce polyploidy and CIN (19–23). On the other hand, mutants of Cdc20 (p55Cdc) with decreased ability to bind to Mad2 failed to respond in SAC arrest (24). By contrast, mutation of the SAC protein kinase domains, which target p55Cdc, was observed in several cancer cell lines (24, 25). SAC proteins are thus necessary for normal chromosomal segregation, and reduction of their function induces carcinogenesis. For instance, decreasing activity of SAC members BubR1 (19, 21), Bub3 (20), and Mad2 (22) increases the carcinogenic properties of normal cells.

Moreover, reduction or mutation of SAC proteins may weaken the effects of tubulin-binding agents toward cancer cells (26, 27). Although the activation of SAC proteins occurs through tubulin-binding agents in both normal and cancer cells, SAC activity is not sustained for a prolonged period except in normal cells (24, 28). Inadequate progression of anaphase from metaphase is known as "adaptation." Dysfunction of SAC in cancer cells causes adaptation. Additionally, it is suggested that SAC proteins regulate the cell death at the M phase in a process called mitotic catastrophe (28–30). Therefore, these

proteins are important for inducing apoptosis caused by tubulin-binding drugs.

In this study, we analyzed the mechanism of antitumor activity of QO-1 in cancer cell lines to determine if the compound exerts the activity via cell cycle regulation and SAC proteins and also if it could directly attack microtubules.

Materials and Methods

Reagents

All cultures and reagents were purchased from Sigma (St. Louis, MO, USA), unless otherwise indicated. Macarpine and QO-1 were chemically synthesized by Ishikawa et al. (1, 2). Macarpine, QO-1, paclitaxel (TAX), vinblastine (VBL), and vinorelbine (VNR) (Wako Pure Chemical Industry, Osaka) were dissolved in and diluted with dimethyl sulfoxide (DMSO) and stored at -20°C at a concentration of 5 mM. Antibodies used in this study were given in the sections on western blotting and immunofluorescence.

Cell lines and culture conditions

The Mes13 cell line (derived from mouse kidney cell) was kindly provided by Dr. I. Ishii (Chiba University). All other cell lines were purchased from ATCC (Manassas, VA, USA), unless otherwise indicated. As cancer cell lines, we used 15 cell lines. Caki-1 (human kidney cancer cell line) was grown in McCoy's 5A (Wako). HeLa (human cervical cancer cell line), obtained from RIKEN (Tsukuba); A498 and 786-O (human kidney cancer); and A549, PCP, and PC14 (human lung cancer) were grown in DMEM (Wako). MCF-7 and MDA-MB-423 (human breast cancer); KLM-1, Paca2, and PANC-1 (human pancreas cancer); DU-145 and PC3 (human prostate cancer); and HCT-15 (human colon cancer) were grown in RPMI1640 (Wako). As non-tumor cell lines, we used Mes-13 and Met-5A (human mesothelial cell line). Mes-13 was grown in DMEM supplemented with 0.01 M HEPES buffer solution and Met-5A was grown in RPMI1640-Glutamax (Gibco BRL, Langley, OK, USA). All cells were cultured with 10% fetal bovine serum (FBS) (Equitech-Bio, Kerrville, TX, USA), 1.0 units/ml penicillin (Gibco BRL), and 2.0 mg/ml streptomycin (Gibco BRL) at 37°C in atmosphere with 5% CO_2 .

Cytotoxicity assay (MTT assay)

To compare QO-1 activity with the parental compound macarpine, 3.0×10^3 MCF-7 cells were seeded in each well of a 96-well plate. After 24-h incubation, an optimum concentration gradient of macarpine and QO-1 were added to each well, followed by culturing for 48 h.

Finally, to assess the sensitivity of the cells to these compounds, cell viability was assessed using the proliferation reagent 3-(4,5-dimethyl thiazoyl-2-yl)-2,5-diphenyltetrazolium bromide (MTT) (Dojindo, Kumamoto), according to the manufacturer's instructions. Control cells were treated with 0.1% DMSO, which is the vehicle for these compounds. On the other hand, QO-1 activity was also assayed against other cell lines, totally 22 (20 cancer cell lines and 2 non-cancerous cell lines) cell lines. IC_{50} values were calculated by GraphPad Prism 5J software (GraphPad Software, Inc., La Jolla, CA, USA).

Cell cycle analysis

A total of 2.0×10^5 cells were seeded in 60-mm dishes and cultured for 24 h. The cells were then cultured with QO-1 (at IC_{50} value for each cell line). After incubation for each indicated period, the cells were fixed in 80% ethanol (Wako) and incubated for 30 min at room temperature in PBS containing 50 $\mu\text{g}/\text{ml}$ propidium iodide (Wako), 2.8% FBS, 0.01% sodium azide (Wako), and 200 $\mu\text{g}/\text{ml}$ RNase A. Finally the cell suspension was filtered with a nylon mesh filter, and the filtrate was analyzed using a MoFlo cell sorter (Dako, Tokyo).

Western blotting analysis

A total of 1.0×10^6 HeLa or MCF-7 cells were seeded in 60-mm dishes and cultured for 24 h. Cells were collected by scraping and then dissolved in ice-cold lysis buffer [50 mM Tris-HCl (pH 6.5), 10% glycerol, 10% β -mercaptoethanol (Wako), 0.5 mM phenylmethane sulfonyl fluoride (PMSF) solution, 2% sodium dodecyl sulfate (SDS) (Wako), 1 mM sodium orthovanadate, and 1% protease inhibitor cocktail]. Each sample, including 20 μg of protein, was electrophoresed through a 5% or 10% SDS-polyacrylamide (Wako) gel and transferred to a polyvinylidene difluoride (PVDF) membrane (Atto Corp., Tokyo). The membranes were blocked with Tris-buffered saline – 0.1% TBS-T [13.7 mM NaCl (Wako), 2.5 mM Tris, 0.05% Tween20 (Wako)] containing 0.3% skim milk (Yukijirushi, Tokyo). The membranes were then subjected to immunoblotting with each polyclonal antibody for Bub1 (1:1000; Abcam, Cambridge, UK), Mad2 (1:1000, Abcam), Bax (1:1000; Cell Signaling Technology, Beverly, MA, USA), Bcl-2 (1:200, N-19: sc-492; Santa Cruz Biotechnology, Santa Cruz, CA, USA), cyclin B1 (1:200, Santa Cruz Biotechnology), β -actin (1:2000), goat anti-mouse IgG-HRP, and donkey anti-rabbit IgG-HRP (Santa Cruz Biotechnology). These antibodies were diluted with Immuno Enhancer (Wako) or TBS-T containing 0.1% skim milk. Detection was accomplished using Immobilon Western (Millipore, Tokyo) and was detected by LAS-1000 Plus (Fuji Film, Tokyo). Protein bands were measured by Scion Image

(Scion; <http://www.scioncorp.com>). Each protein density value was normalized to β -actin.

In vitro microtubule polymerization assay

Microtubule polymerization was determined using a tubulin polymerization assay kit (Cytoskeleton, Denver, CO, USA) according to the vendor's instructions. Microtubule proteins (1.0 mg/ml tubulin) were suspended in PEM buffer (80 mM Na-PIPES pH 6.9, 1 mM MgCl_2 , and 1 mM EGTA), used as a tubulin working buffer as a form of G-PEM (PEM buffer plus 1.0 mM GTP). Microtubule polymerization dynamics was monitored by measuring the change in absorbance at 340 nm every 1 or 5 min for 60 min at 37°C using a SmartSpec™ 3000 (Bio-Rad Laboratories, Hercules, CA, USA). As positive controls of the microtubule sensitizer, TAX and VNR were prepared, of which concentrations were set according to previous reports (31, 32).

In vivo tubulin polymerization assay

A total of 1.0×10^6 of MCF-7 cells were seeded in 60-mm dishes. After 24 h, cells were cultured with or without QO-1 (0.2 μM) or vinorelbine (25 nM) or paclitaxel (25 nM) for another 24 h. Cells were washed with warmed PBS, collected by scraping, and then dissolved in microtubule stabilization buffer [20 mM Tris-HCl (pH 6.8), 1 mM MgCl_2 , 2 mM EGTA, 0.5% Nonidet P-40, 1 mM sodium orthovanadate, 10% glycerol, 2 mM PMSF solution, 0.5% protease inhibitor cocktail, 4 μM paclitaxel]. Next, the collected cells were incubated at 37°C for 5 min and centrifuged at $20,000 \times g$, at 20°C, for 10 min. The supernatant was used as soluble (non-polymerized) tubulin. On the other hand, the pellet was added with ice-cold lysis buffer (the same one as used in the "western blotting analysis" method) and the lysate was processed by the protocol to obtain polymerized tubulin. After that, electrophoreses and transfer to membranes were done according to the "western blotting analysis" protocol. The membranes were then subjected to immunoblotting with the primary antibody Rat Anti Tubulin α (MCA78G) (Serotec, Oxford, UK) (1:5000) for microtubules, using the secondary antibody Anti-rat IgG-HRP-linked Antibody (7077) (Cell Signaling Technology) (1:3000).

Caspase assay

Caspase activity was measured with Caspase-Glo 3/7 and Caspase-Glo 8 assay kits (Promega, Tokyo) according to the manufacturer's instructions. HeLa and MCF-7 cells were treated with QO-1, VBL, and TAX and were assayed at different time points. Each concentration was used at the IC_{50} . Control cells were treated with DMSO. The luminescence of the samples was measured in a

Turner Designs Luminometer Model TD-20/20 Genetic Reporter Instrumentation Package for Stabilized Assays (Promega).

Immunofluorescence microscopic observation

Briefly, a total of 9.0×10^4 MCF-7 cells were seeded on the coverslips for the experiment. After 24 h, QO-1 (IC_{50}) or 25 nM vinorelbine (as a positive control) were added. When the culture reached each time point, cells were washed in pre-warmed PBS and fixed with 4% paraformaldehyde for 20 min at room temperature. Fixed cells were washed, pre-incubated with 3% BSA in 0.1% Saponin/PBS(−) as a blocking step, and then incubated with each primary antibody, followed by a secondary antibody, if needed. Rat Anti Tubulin α (MCA78G) (Serotec) antibody (1:1000) was used as the primary antibody to identify microtubules, followed by the secondary antibody Alexa Fluor® 488 Anti-rat IgG (goat) (A21208) (Invitrogen, Carlsbad, CA, USA) antibody (1:1000). Finally, to detect the nucleus, coverslips were treated with RNaseA (100 $\mu\text{g}/\text{ml}$), PI (50 $\mu\text{g}/\text{ml}$) in PBS(−) for 30 min. After washing, coverslips were mounted on glass slides and both fluorescence and Nomarski photomicrographs were taken using a confocal microscope (FV500; Olympus, Tokyo).

Statistical analysis

The data were analyzed with one-way analysis of variance, followed by Student's *t*-test, Dunnett's test, or Tukey-Kramer test. A *P*-value of less than 0.05 was considered significant.

Results

Anti-proliferation effect of QO-1 compared to macarpine

QO-1, which are the compounds derived from macarpine (see structures in Fig. 1A), inhibited cell proliferation in a concentration-dependent manner in MCF-7 cells. The effect of QO-1 was significantly more potent than macarpine at the respective concentrations (Fig. 1B). Moreover, QO-1 also caused concentration-dependent growth inhibition against 19 of 20 cancer cell lines including MCF-7 (Table 1). In only MIA Paca2, one of the pancreatic cancer cell lines, QO-1 showed no cytotoxic effect. On the other hand, QO-1 was also tested in non-cancerous cells. Met-5A was resistant to QO-1 even at high concentrations, although the Mes-13 growth was inhibited by QO-1 in concentration-dependent manner (Table 1).

In particular, these compounds effectively and reproducibly attacked HeLa (IC_{50} : QO-1, 0.10 μM) and MCF-7 (IC_{50} : QO-1, 0.20 μM) cells. As shown in Table 1, there

Table 1. IC₅₀ values of QO-1 against 22 cell lines

Cell line	Origin	IC ₅₀ (μM)
HeLa	Cervical	0.104
Caki-1	Kidney	0.598
786-O	Kidney	0.282
A549	Lung	0.425
PCP	Lung	0.073
PC14	Lung	0.097
MIA PaCa2	Pancreas	N/A
PaCa2	Pancreas	0.169
KLM-1	Pancreas	0.091
PANK-1	Pancreas	0.060
DU-145	Prostate	0.023
LNCaP	Prostate	0.005
PC3	Prostate	0.319
MDA-MB-423	Breast	0.384
MCF-7	Breast	0.196
H28	Mesothelial cell	5.778
H2052	Mesothelial cell	0.535
MSTO-211H	Mesothelial cell	0.377
DLD-1	Colon	0.063
HCT-15	Colon	0.055
Mes13	Kidney	0.266
Met-5A	Mesothelial cell	N/A

IC₅₀ values of QO-1 against 22 cell lines (20 cancer cells and 2 non-cancerous cells: Mes13 and Met-5A) were treated with QO-1 for 48 h then cell viabilities were determined by the MTT assay as described in Materials and Methods. Using the combined results from at least three independent experiments for each cell line, the IC₅₀ values were calculated by GraphPad Prism 5J software. "N/A" means it was impossible to determine the value because the cell viabilities were over 50%.

were also other cell lines that seemed to be quite sensitive to QO-1. However, on the other hand, we previously checked if QO-1 might affect the cell cycle in HeLa and MCF-7 cells (unpublished data). So we chose these two cell lines to investigate the functional mechanism of QO-1.

QO-1-induced G₂/M phase arrest

To investigate the mechanism of QO-1-induced growth inhibition, we next determined if QO-1 affected the progression of the cell cycle using flow cytometry. The distribution of the whole cell population after exposure to QO-1 is shown in Fig. 2. Also we looked at the sub-G₁ phase and G₂/M phase population (Tables 2 and 3), which were the phases affected by QO-1. In QO-1-treated cells,

the G₁ population gradually shrunk and then slightly grew from 24 to 48 h exposure to QO-1 (Fig. 2). In contrast, the G₂/M population immediately grew and then shrank sharply from 24 to 48 h exposure to QO-1 both in HeLa (Table 2, upper line) and MCF-7 cells (Table 3, upper line). It suggests that G₂/M arrest had occurred, but some mitotically exited cells continued progression and entered a second round of DNA replication (adaptation). On the other hand, the sub-G₁ population, which is a marker of apoptosis, started to increase with a disappearance of the G₂/M population both in HeLa (Table 2, lower line) and MCF-7 cells (Table 3, lower line).

The SAC proteins induced by QO-1

Compared with control cells (Fig. 3A, left), it was observed that expression of Bub1, a member of the SAC protein family, synchronously increased with the growth of the G₂/M population (Fig. 2) by QO-1 exposure (Fig. 3A, right). It reached the peak around 8 to 20 h after exposure in both cell lines (Fig. 3B, left), but on the other hand, Mad2, which is complexed with p55Cdc, was almost stable in this study (Fig. 3: A and B, right). To examine the progression from the G₂ to M phase in detail, we also checked cyclin B1 expression. It is ubiquitinated via APC/C^{Cdc20} during progression from M to the next G₁ phase, so protecting cyclin B1 from degradation is important to maintain the mitotic state. In both HeLa and MCF-7 cells, expression of cyclin B1 was gradually up-regulated around 8 to 24 h after QO-1 exposure (Fig. 3A, right). Additionally, cyclin B1 expression disappeared after 48 h exposure to QO-1 in both cells (Fig. 3A, right). This result indicates the possibility of mitotic exit, which agrees with the flow cytometry results of 48 h where the G₂/M phase population was decreased compared to 24 h.

Effect of QO-1 on microtubule polymerization

Because QO-1 induced M-phase arrest, we determined if QO-1 could directly affect microtubule polymerization. QO-1 did not increase microtubule polymerization, in contrast to paclitaxel that promotes microtubule polymerization (Fig. 4A). On the other hand, a microtubule-depolymerizing agent, vinorelbine, inhibited microtubule polymerization at 37°C where the polymerization was considered to increase automatically. QO-1 also exhibited half the inhibitory effect of vinorelbine against microtubule polymerization (Fig. 4B). Moreover, the *in vivo* polymerization study revealed that QO-1 also increases the ratio of soluble tubulin (non-polymerized tubulin) as vinorelbine did in the cellular environment, although paclitaxel increased the ratio of polymerized tubulin as expected (Fig. 4: C, D).

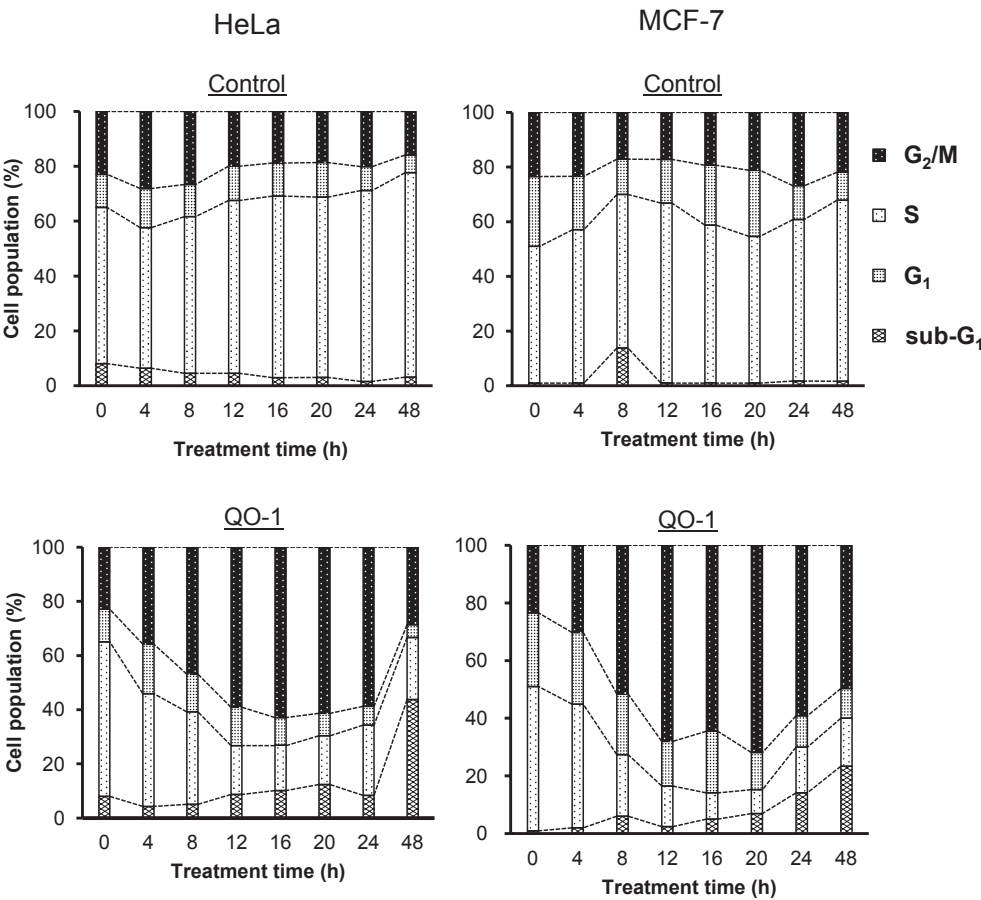


Fig. 2. QO-1-induced perturbation of cell cycle progression of HeLa and MCF-7 cells. Effect of QO-1 (HeLa, 0.10 μ M; MCF-7, 0.20 μ M) on cell cycle progression. Columns represent the mean value of relative percentage of cells in each cell cycle phase over the time course of QO-1 treatment. Data are from three independent experiments.

Table 2. Transition of G₂/M and sub-G₁ population in HeLa cells

Time (h)		0	4	8	12	16	20	24	48
Control	G ₂ /M (%)	22.9	28.1	26.7	20.0	18.6	18.4	20.2	15.9
	S.D.	3.1	5.2	4.4	3.5	0.6	0.4	1.8	3.7
QO-1	G ₂ /M (%)	-	35.1	46.7	61.0 ^{*,++}	62.9 ^{***,++}	61.8 ^{*,++}	58.7 [*]	28.8 ⁺
	S.D.	-	2.5	5.0	6.7	10.5	14.8	29.5	8.9
Control	sub-G ₁ (%)	8.0	6.3 [*]	4.3 ^{***}	4.5 ^{***}	4.0 ^{***}	4.1 ^{***}	1.6 ^{***}	3.1 ^{***}
	S.D.	0.4	0.9	0.2	0.4	0.3	0.9	0.2	1.2
QO-1	sub-G ₁ (%)	-	6.5	5.7	5.7	10.3 ⁺	12.0	8.3 ⁺⁺	43.9 ^{***,+}
	S.D.	-	1.3	1.6	1.0	2.6	3.1	0.4	17.1

Data show the mean of three independent experiments. * $P < 0.05$, *** $P < 0.001$ vs. each “Control 0 h”, Dunnett’s test. ⁺ $P < 0.05$, ⁺⁺ $P < 0.01$ vs. each “Control” at the same time point, Student’s *t*-test.

Apoptosis pathways induced by QO-1

The Bcl-2 family is known as a crucial regulator of apoptosis. Phosphorylation of Bcl-2 is induced on serine residues in tumor cells arrested by microtubule-targeting drugs (33), which is associated with inactivation of its anti-apoptotic function. In both HeLa and MCF-7 cells, phospho-Bcl-2 expression was observed by 24-h expo-

sure to QO-1 (Fig. 5A, upper bands of Bcl-2). On the other hand, Bax, known as a pro-apoptotic protein belonging to the Bcl-2 family, seemed to increase during 48-h exposure to QO-1 in MCF-7 cells (Fig. 5A, right). Bax induces the release of downstream factors such as cytochrome *c* that leads to activation of caspase-3, the key executioner of apoptosis. We investigated if cell

Table 3. Transition of G₂/M and sub-G₁ population in MCF-7 cells

Time (h)		0	4	8	12	16	20	24	48
Control	G ₂ /M (%)	23.5	30.4	29.3	19.8	24.3	25.5	26.9	21.9
	S.D.	1.1	11.1	10.2	5.2	7.5	4.2	5.5	1.2
QO-1	G ₂ /M (%)	-	40.8*	57.6***	70.6***,+++	68.8***,+	75.0***,++	59.1***,+	49.7***,++
	S.D.	-	5.9	3.2	3.1	9.5	7.0	1.4	8.5
Control	sub-G ₁ (%)	0.9	1.6	7.1	3.0	1.9	2.5	1.7	1.6
	S.D.	0.1	1.0	5.8	3.0	1.1	2.6	0.7	0.8
QO-1	sub-G ₁ (%)	-	2.2	1.7	4.6	4.0	5.5*	14.3***,++	23.4***,++
	S.D.	-	1.3	1.5	3.5	1.2	1.8	0.4	2.3

Data show the mean of three independent experiments. * $P < 0.05$, *** $P < 0.001$ vs. each "Control 0 h", Dunnett's test. + $P < 0.05$, ++ $P < 0.01$, +++ $P < 0.01$ vs. each "Control" at the same time point, Student's *t*-test.

death involved the caspase pathway. Similar to paclitaxel, QO-1 was found to activate caspase-3/7 in HeLa cells (Fig. 5B), although it did not in MCF-7 cells, which are known to have mutant caspase-3 (data not shown).

Abnormal mitosis and apoptotic-like shape of cells induced by QO-1

After exposure to QO-1, the cell morphology showed abnormal mitosis. To confirm the effect of QO-1 on microtubules in cells, we finally the visualized cellular spindle apparatus, which is composed of microtubules (Fig. 5C). Microtubules were stained green (Alexa Fluor® 488 conjugate) and DNA was stained red using PI.

Confocal micrographs of control cells showed normal radial arrays of microtubules in interphase cells (Fig. 5C: a, b) and typical mitotic process (Fig. 5C: c). On the other hand, QO-1-treated cells had abnormal multipolar spindles after 16-h exposure (Fig. 5C: e). There were also multinucleated cells treated with QO-1 for 16 h (Fig. 5C: f) and 48 h (Fig. 5C: l), similar to those treated with vinorelbine (Fig. 5C: m), which might result from an abnormal multipolar mitosis. Moreover, abnormal chromosomes that failed to make chromosomal pairs and several fragmented DNA pieces and clusters were observed at 16 h (Fig. 5C: d), 24 h (Fig. 5C: g, h), and 48 h (Fig. 5C: j) after QO-1 exposure, similar to those treated with vinorelbine (Fig. 5C: m, n).

Discussion

It has been known that organic structures with a naphthoquinone 1-oxime core, which is found in QO-1, exert antiviral activity. In this study, QO-1 showed cytotoxic activity in a wide variety of cancer cell lines. It also attacked normal cells, like Mes-13 cells, but the effect was mild on Met-5A cells. The significant difference between these two types of was the growth rate; Mes-13 cells

grew fast and Met-5A cell grew slowly. Because it attacks tubulin, like vinca alkaloids do, QO-1 is expected to affect multiply proliferating cells. Thus the above difference is derived from the growth rate of each cell line.

QO-1 increased the number of cells in the G₂/M population with a peak at 8 to 20 h (Fig. 3A). Thus QO-1 displayed the pharmacological activity of a microtubule-depolymerization agent. This suggests that the cytotoxic activity of QO-1 might derive from mitotic arrest. Duration of mitosis does not dictate subsequent cell fate like cell death, but activation of SAC that leads to mitotic arrest is required whether a cell dies in mitosis or dies in the subsequent interphase (34). To clarify the SAC involvement in QO-1-induced cell death, we examined the change of SAC proteins, Bub1 and Mad2, over time. After QO-1 exposure, expression of Bub1 greatly increased from 8 to 20 h and then disappeared or became very weak at 48 h (Fig. 3), concomitantly with G₂/M-phase arrest as analyzed by flow cytometry (Fig. 2 and Tables 2 and 3). However, the expression of the other SAC protein, Mad2, did not change. To explain the above results, the following reason was suggested: Mad2 makes a complex with p53Cdc, which is a direct activator of APC/C. Even if QO-1 did not affect Mad2 expression, there would still be a possibility to affect its complex, so further study to detect the factors that make the complex like p53Cdc or activation of APC/C is needed. On the other hand, SAC activation correlates with a significant increase in the concentration of SAC proteins at kinetochores (11). So detecting the localization of SAC expression at kinetochores will help to assess how long SAC activation is maintained by QO-1. Actually, a specific marker of mitotic arrest (cyclin B1 accumulation) was observed after QO-1 exposure, like that observed with the tubulin-binding agent paclitaxel (Fig. 3A). Cyclin B1 is a necessary factor to maintain mitosis, and also it is considered that delaying cyclin B1 degradation allows

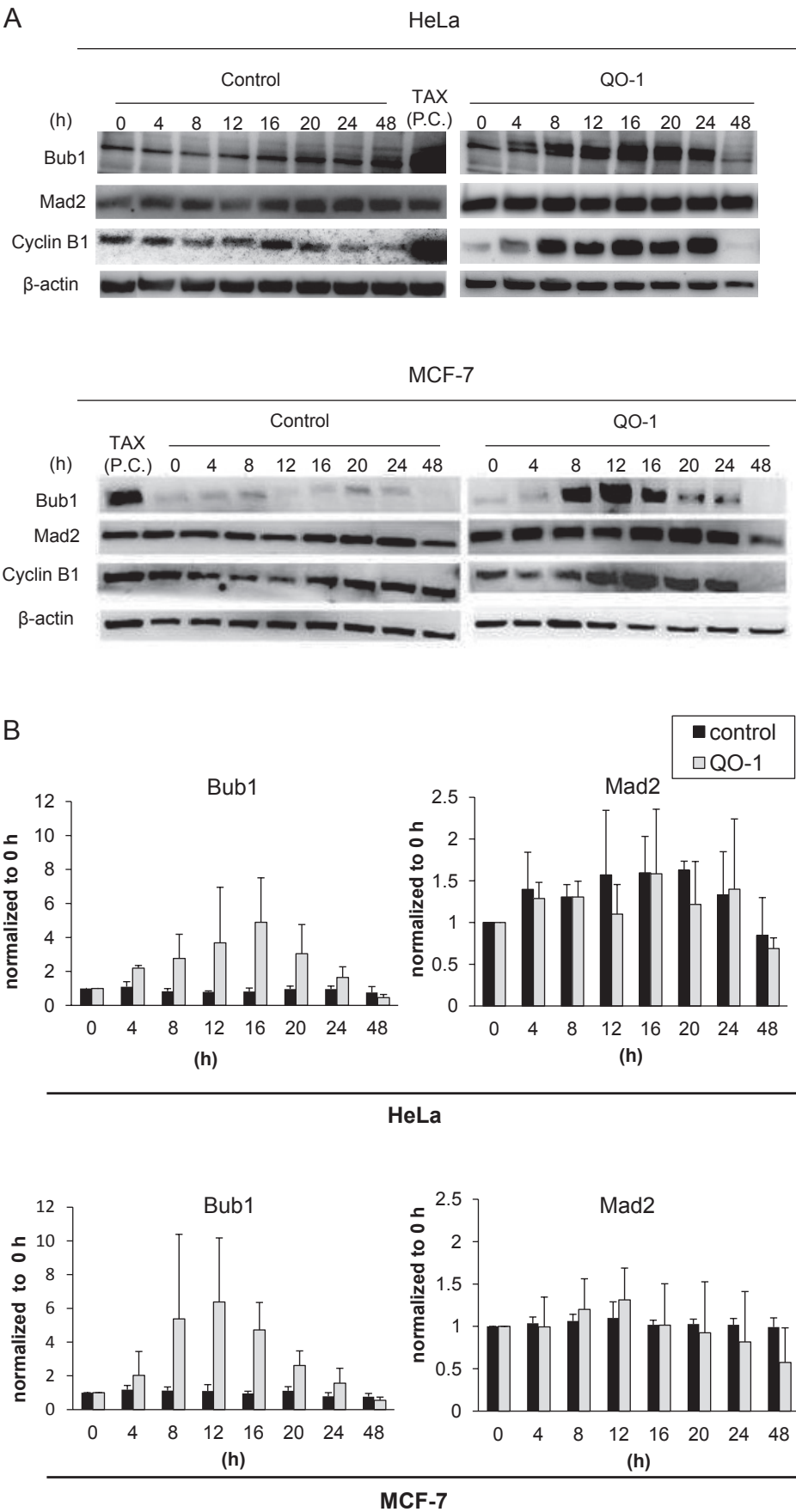
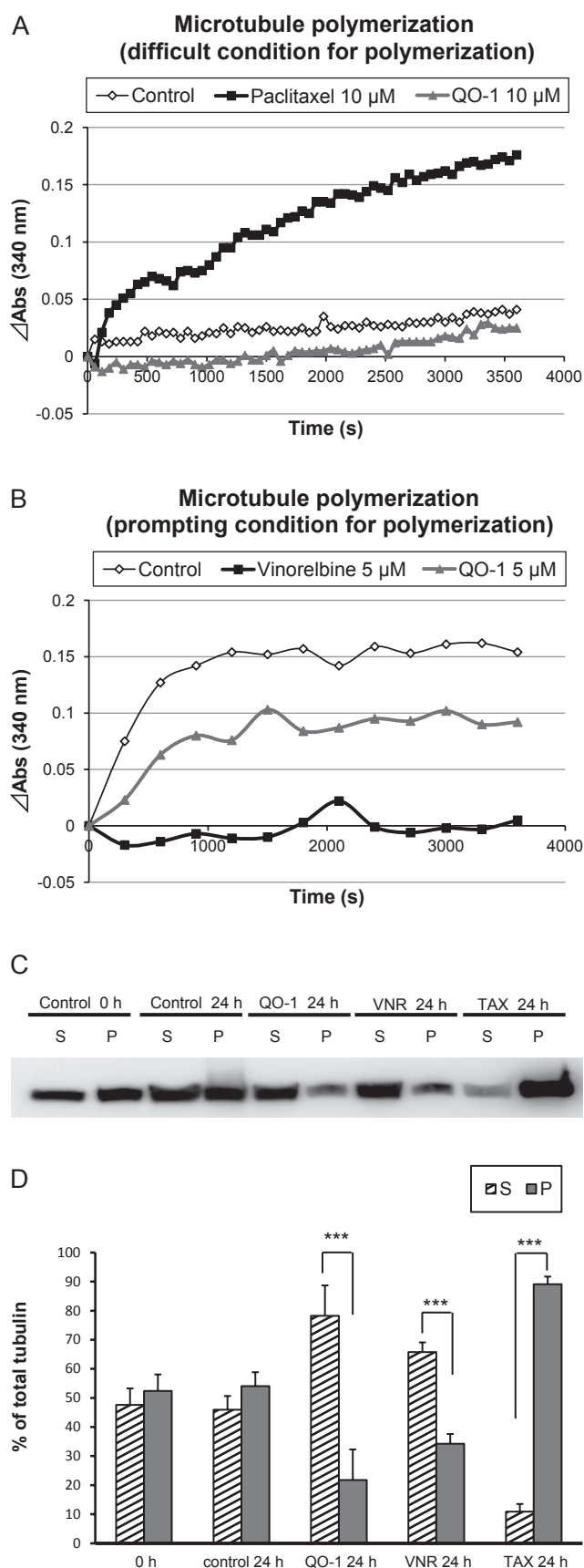


Fig. 3. Effect of QO-1 on SAC proteins Bub1 and Mad2 and cell cycle regulator protein cyclin B1 in HeLa and MCF-7 cells. Cells were treated with the vehicle or with QO-1 (HeLa, 0.10 μ M; MCF-7, 0.20 μ M) for the indicated time. Paclitaxel (TAX) at 50 nM was used as a positive control. After exposure to QO-1 for the indicated periods, protein expressions of Bub1, Mad2, cyclin B1, and β -actin were analyzed by western blotting as described in Materials and Methods. β -Actin was used as an internal standard. A: Representative photos of Bub1, Mad2, and cyclin B1 in HeLa and MCF-7 cells. B: Transitional change of Bub1 and Mad2 in HeLa and MCF-7 cells. Data shown are each the mean \pm S.D. of three independent experiments.



more time for the death signal to accumulate (34). Combining the results of cyclin B1 and Bub1 expressions with the flow cytometry data, it was clear that mitotic arrest was maintained until 24-h exposure, although mitotic exit already happened at the 48-h exposure point.

Microscopic morphology of QO-1-treated cells also exhibited typical mitotic arrest (Fig. 5C). If cell death occurs, derived from mitotic arrest, what is the mechanism? There are abundant reports concerning mitotic cell death, although the pathways are not completely merged. Microtubule-active drugs inhibit spindle functions during mitosis and cause M-phase arrest. During M-phase arrest induced by these drugs, p53 is gradually stabilized. It is accompanied by induction of p21, which promotes post-mitotic G₁ arrest (35). Therefore prolonged time in mitosis induces both cell death in mitosis and mitotic exit known as mitotic slippage. In the latter case, slipped-out cells display multinucleated morphology (aneuploidy cells). It is suggested that an excessively huge DNA content eventually accumulates genotoxic stress in the post-mitotic G₁ phase (36), and then p53 responds to DNA damage, triggering apoptosis. Additionally, such slippage cells do not necessarily undergo cell death and some cells may still be alive and remain in interphase or enter a second mitosis (34). On the other hand, high concentrations of vinflunine, one of the vinca alkaloids, characteristically induce a G₂/M block and Bcl-2 phosphorylation, while low concentrations of vinflunine suppress microtubule dynamics and slow down mitotic progression but fail to block cells in the G₂/M, following exit mitosis, a p53-dependent post-mitotic G₁ arrest (37). We observed both mitotic arrested cells and some aneuploidy cells after QO-1 exposure (Fig. 5C: i, l). Addition-

Fig. 4. Effect of QO-1 on tubulin assembly. **A:** Promoting effect on in vitro microtubule polymerization. Paclitaxel was used as a positive control. MAP-rich tubulin (1.0 mg/ml) was incubated at room temperature for 3,600 s, and then the indicated compounds were added at the indicated concentrations. A_{340} values were recorded once per 60 s. The results are presented as the difference of absorbance at each time point. **B:** Inhibitory effect on in vitro microtubule polymerization. Vinorelbine was used as a positive control. MAP-rich tubulin (1.0 mg/ml) was incubated at 37°C for 3,600 s, and then the indicated compounds were added at the indicated concentrations. A_{340} values were recorded once every 300 s. The results are presented as the difference of absorbance at each time point. **C and D:** In vivo microtubule polymerization in HeLa cell. Cells were prepared as described in Materials and Methods. 0 h, cells not treated with any drug; Control 24 h, cells treated with 0.1% DMSO for 24 h; QO-1 24 h, cells treated with QO-1 (0.10 μ M) for 24 h; VNR 24 h, cells treated with vinorelbine (25 nM) for 24 h; TAX 24 h, cells treated with paclitaxel (25 nM) for 24 h. **C:** Representative photos of α -tubulin (component of microtubule). S, soluble (non-polymerized) tubulin; P, polymerized tubulin. **D:** Ratio of soluble tubulin and polymerized tubulin. Data shown are each the mean \pm S.D. of three independent experiments. *** $P < 0.001$ (Student's *t*-test).

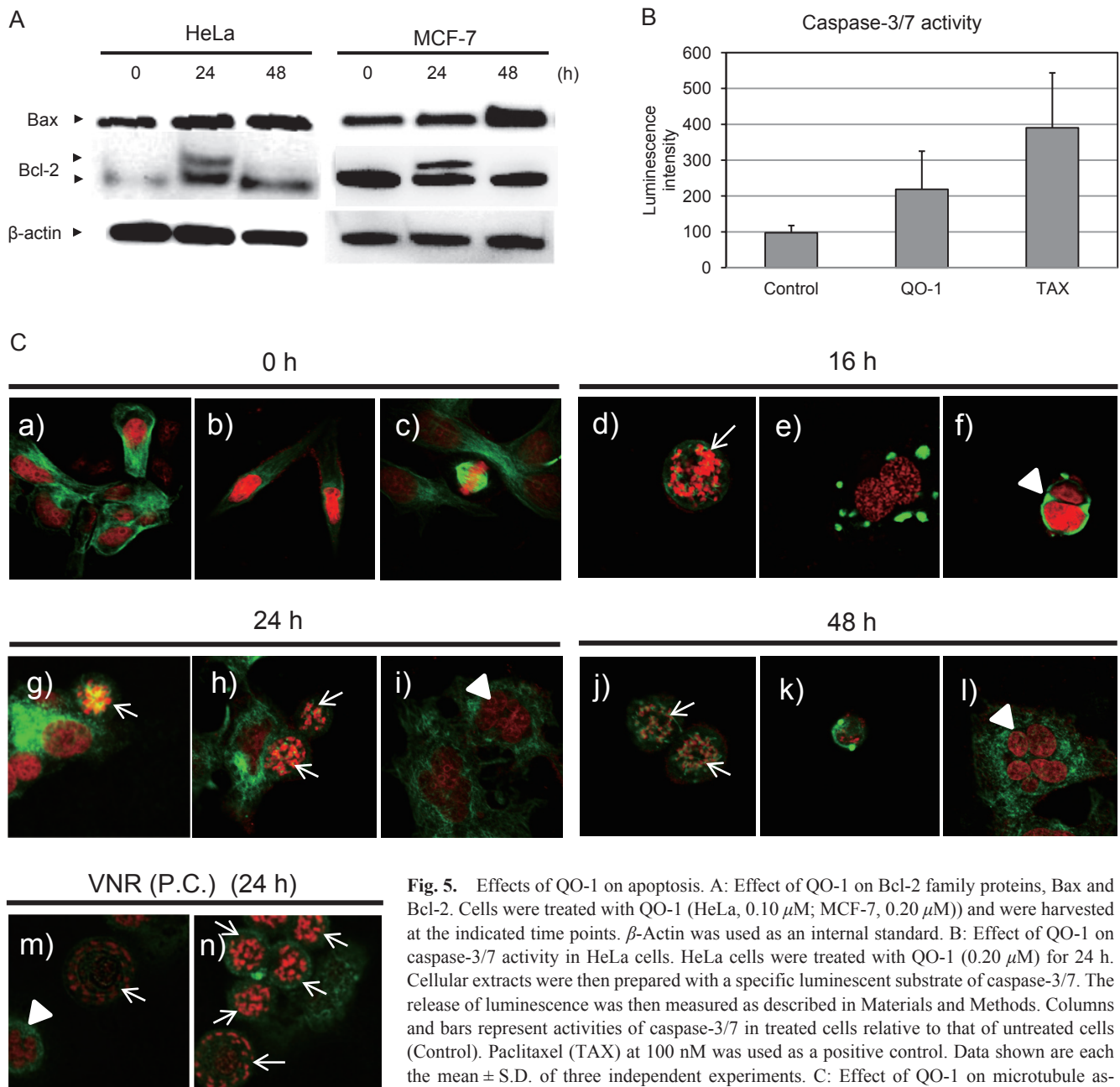


Fig. 5. Effects of QO-1 on apoptosis. **A:** Effect of QO-1 on Bcl-2 family proteins, Bax and Bcl-2. Cells were treated with QO-1 (HeLa, 0.10 μ M; MCF-7, 0.20 μ M) and were harvested at the indicated time points. β -Actin was used as an internal standard. **B:** Effect of QO-1 on caspase-3/7 activity in HeLa cells. HeLa cells were treated with QO-1 (0.20 μ M) for 24 h. Cellular extracts were then prepared with a specific luminescent substrate of caspase-3/7. The release of luminescence was then measured as described in Materials and Methods. Columns and bars represent activities of caspase-3/7 in treated cells relative to that of untreated cells (Control). Paclitaxel (TAX) at 100 nM was used as a positive control. Data shown are each the mean \pm S.D. of three independent experiments. **C:** Effect of QO-1 on microtubule assembly and nucleus morphology undergoing mitosis. Confocal immune-micrographs of microtubules (green) and DNA (red) are shown. MCF-7 cells were observed under a confocal laser microscope ($\times 60$). Cells were treated with or without QO-1 (0.20 μ M) for the indicated time and then harvested. After fixing and incubation with antibodies as described in Materials and Methods, microscopic observation was done. Photographs were representative pictures of QO-1-treated cells (a–l) and vinorelbine-treated cells as a positive control (m, n). White arrowheads indicate multiple nuclei in a cell (f, i, l, and m). White arrows indicate abnormal chromosomes with several fragmented DNA pieces and clusters at metaphase (d, g, h, j, m, and n). “0 h”, “16 h”, “24 h”, and “48 h” indicate cells treated with QO-1 for each time period, and “VNR (P.C.) (24 h)” indicates cells treated with vinorelbine for 24 h, as a positive control.

ally, we observed that the sub-G₁ population grew sharply after QO-1 exposure for 48 h in HeLa cells and also the M-phase population decreased at the same time (Fig. 2 and Tables 2 and 3). At that time, the G₁ population was not so changed compared with that at 24 h (Fig. 2). This indicates the progression from M to the next G₁ phase

might occur at some level, but most of the sub-G₁ population might be derived from cells that directly underwent mitotic cell death under these experimental concentrations. We need further study to confirm which pathway is major.

Mitochondrial Bcl-2 family members have a crucial

role in vinca alkaloids or paclitaxel-induced apoptosis. Although the molecular mechanisms that link mitotic arrest and apoptosis are poorly understood, mitochondria is considered as the point of convergence for the apoptotic signals induced by the vinca alkaloids (37). We examined if Bax and Bcl-2 proteins contribute to apoptosis induced by QO-1. As a result, expression of Bax relatively increased in MCF-7 after exposure to QO-1, and the inactive form of Bcl-2 expression was also increased in both cell lines. So QO-1 might shift the Bcl-2 family balance toward apoptosis.

Finally we determined if the caspase family is involved in QO-1 induced apoptosis. Tubulin-binding agents can induce apoptosis both via a caspase-dependent pathway and caspase-independent pathway (38). For instance, nocodazole induces caspase-dependent apoptosis in some cell lines (39, 40). Caspase-3 activation can lead to cleavage of BubR1 before nocodazole-induced apoptosis (41). Vice versa, the cleavage of Bub1 is necessary for apoptosis via a caspase pathway in HeLa and MCF-7 cells (42). In this study, QO-1 induced similar microtubule-depolymerization effects as nocodazole does. Hence, QO-1 was expected to induce apoptosis after degradation of SAC proteins like nocodazole does. As mentioned above, the sub-G₁ population grew after the G₂/M population shrunk (Fig. 2), and Bub1 expression decreased or disappeared at the time point of sub-G₁ increase (Fig. 3). These results support the above assumption about apoptosis being induced by QO-1. Like paclitaxel, QO-1 activated caspase-3/7 in HeLa cells but not in MCF-7 cells. This suggested that QO-1-induced apoptosis occurs via different pathways in each cell line. Although caspase-3 is commonly activated by numerous death signals, it is not expressed in the MCF-7 cell line. This cell line is known to undergo cell death in response to stimulation by TNF- α , staurosporine, and other agents. Those previous findings suggested that caspase-3 is necessary for apoptosis-induced nuclear events and DNA fragmentation, but may not be essential for cell death itself. Kagawa et al. showed Bax overexpression induced apoptosis in MCF-7 cells, while restoration of caspase-3 did not affect cell death induced by Bax (43). Although the precise mechanism is not yet clear, it is certain that some apoptotic events occurred in MCF-7 cells in the absence of caspase-3. The mechanism that compensates for the absence of caspase-3 function in MCF-7 cells needs further clarification. Moreover, previously it was found that a caspase inhibitor allowed mitotic cells more time for slippage and reduced the number of cell deaths in mitosis (34). Gascoigne et al. speculated that cell fate is dictated by two competing but independent mechanisms, one involving caspase activation and the other is protecting cyclin B1 from degradation (34). Therefore our results of

cyclin B1 accumulation and activation of caspase 3 (in HeLa cells) are consistent with the previous reports.

Above all, we found that QO-1 exerted growth inhibition and cytotoxicity, which partly derived from its inhibiting activity on microtubule polymerization and following activation of SAC. Despite these findings, the precise mechanism remains unclear. A possibility was suggested that SAC activation by QO-1 might induce apoptotic factors. Activation of SAC proteins and following events via the Bcl-2 family or caspase-3/7 might result in potent apoptosis. Further studies are needed, but QO-1 activity revealed not only its promising effect but also proves the common core structure of such compounds to be a valuable innovation for applicable antitumor active seed compounds.

Acknowledgments

We thank Dr. Yuji Nakayama (Chiba University) for his valuable advice and assistance in performing the cell cycle analysis. We also appreciate Dr. Itsuko Ishii (Chiba University) for providing us with the Mes-13 cell line. This study was partly supported by a Grant-in-Aid for Young Scientists (start-up) from the Japan Society for the Promotion of Sciences and Special Funds for Education and Research (Development of SPECT probes for Pharmaceutical Innovation) from the Ministry of Education, Culture, Sports, Science and Technology, Japan, and a research grant from The Uehara Memorial Foundation.

References

- 1 Ishikawa T, Saito T, Ishii H. Synthesis of macarpine and its cytotoxicity: toward a synthetic route for 12-alkoxybenzo[c]phenanthridine alkaloids through aromatic nitrosation under basic condition. *Tetrahedron*. 1995;51:8447–8458.
- 2 Ishikawa T, Saito T, Ohashi Y, Yoshino R, Kurosawa A, Watanabe T, et al. 2-Aryl-1,4-naphthoquinone-1-oximes: their cytotoxic activity. *Chem Pharm Bull (Tokyo)*. 2011;59:472–475.
- 3 Ishikawa T, Watanabe T, Tanigawa H, Saito T, Kotake TI, Ohashi Y, et al. Nitrosation of phenolic substrates under mildly basic conditions: selective preparation of *p*-quinone monooximes and their antiviral activities. *J Org Chem*. 1996;61:2774–2779.
- 4 Noble RL, Beer CT, Cutts JH. Further biological activities of vincleukoblastine: an alkaloid isolated from *Vinca rosea* (L.). *Biochem Pharmacol*. 1958;1:347–348.
- 5 Wani MC, Taylor HL, Wall ME, Coggon P, McPhail AT. Plant antitumor agents. VI. The isolation and structure of taxol, a novel antileukemic and antitumor agent from *Taxus brevifolia*. *J Am Chem Soc*. 1971;93:2325–2327.
- 6 Muhlradt PF, Sasse F. Epithilone B stabilizes microtubuli of macrophages like taxol without showing taxol-like endotoxin activity. *Cancer Res*. 1997;57:3344–3346.
- 7 Cortes J, O'Shaughnessy J, Loesch D, Blum JL, Vahdat LT, Petrakova K, et al; EMBRACE (Eisai Metastatic Breast Cancer Study Assessing Physician's Choice Versus E7389) Investigators. Eribulin monotherapy versus treatment of physician's choice in patients with metastatic breast cancer (EMBRACE): a phase 3 open-label randomised study. *Lancet*. 2011;377:914–923.
- 8 Hoyt MA, Totis L, Roberts BT. *S. cerevisiae* genes required for

- cell cycle arrest in response to loss of microtubule function. *Cell*. 1991;66:507–517.
- 9 Li R, Murray AW. Feedback control of mitosis in budding yeast. *Cell*. 1991;66:519–531.
 - 10 Jackson JR, Patrick DR, Dar MM, Huang PS. Targeted anti-mitotic therapies: can we improve on tubulin agents? *Nat Rev Cancer*. 2007;7:107–117.
 - 11 Musacchio A, Salmon ED. The spindle-assembly checkpoint in space and time. *Nat Rev Mol Cell Biol*. 2007;8:379–393.
 - 12 Tang Z, Shu H, Oncel D, Chen S, Yu H. Phosphorylation of Cdc20 by Bub1 provides a catalytic mechanism for APC/C inhibition by the spindle checkpoint. *Mol Cell*. 2004;16:387–397.
 - 13 Luo X, Tang Z, Rizo J, Yu H. The Mad2 spindle checkpoint protein undergoes similar major conformational changes upon binding to either Mad1 or Cdc20. *Mol Cell*. 2002;9:59–71.
 - 14 Sironi L, Mapelli M, Knapp S, De Antoni A, Jeang KT, Musacchio A. Crystal structure of the tetrameric Mad1-Mad2 core complex: implications of a ‘safety belt’ binding mechanism for the spindle checkpoint. *EMBO J*. 2002;21:2496–2506.
 - 15 De Antoni A, Pearson CG, Cimini D, Canman JC, Sala V, Nezi L, et al. The Mad1/Mad2 complex as a template for Mad2 activation in the spindle assembly checkpoint. *Curr Biol*. 2005;15:214–225.
 - 16 Boveri T. Zur Frage der Entstehung maligner Tumoren. Jena: Gustav Fischer; 1914. p. 64. (in German)
 - 17 Sasaki M, Sugimoto K, Tamayose K, Ando M, Tanaka Y, Oshimi K. Spindle checkpoint protein Bub1 corrects mitotic aberrancy induced by human T-cell leukemia virus type I Tax. *Oncogene*. 2006;25:3621–3627.
 - 18 Suijkerbuijk SJ, Kops GJ. Preventing aneuploidy: the contribution of mitotic checkpoint proteins. *Biochim Biophys Acta*. 2008;1786:24–31.
 - 19 Baker DJ, Jeganathan KB, Cameron JD, Thompson M, Juneja S, Kopecka A, et al. BuR1 insufficiency causes early onset of aging-associated phenotypes and infertility in mice. *Nat Genet*. 2004;36:744–749.
 - 20 Babu JR, Jeganathan KB, Baker DJ, Wu X, Kang-Decker N, van Deursen JM. Rae1 is an essential mitotic checkpoint regulator that cooperates with Bub3 to prevent chromosome missegregation. *J Cell Biol*. 2003;160:341–353.
 - 21 Dai W, Wang Q, Liu T, Swamy M, Fang Y, Xie S, et al. Slippage of mitotic arrest and enhanced tumor development in mice with BubR1 haploinsufficiency. *Cancer Res*. 2004;64:440–445.
 - 22 Michel LS, Liberal V, Chatterjee A, Kirchwegger R, Pasche B, Gerald W, et al. MAD2 haplo-insufficiency causes premature anaphase and chromosome instability in mammalian cells. *Nature*. 2001;409:355–359.
 - 23 Putkey FR, Cramer T, Morphew MK, Silk AD, Johnson RS, McIntosh JR, et al. Unstable kinetochore-microtubule capture and chromosomal instability following deletion of CENP-E. *Dev Cell*. 2002;3:351–365.
 - 24 Wang X, Jin DY, Wong YC, Cheung AL, Chun AC, Lo AK, et al. Correlation of defective mitotic checkpoint with aberrantly reduced expression of MAD2 protein in nasopharyngeal carcinoma cells. *Carcinogenesis*. 2000;21:2293–2297.
 - 25 Johnson VL, Scott MI, Holt SV, Hussein D, Taylor SS. Bub1 is required for kinetochore localization of BubR1, Cenp-E, Cenp-F and Mad2, and chromosome congression. *J Cell Sci*. 2004;117:1577–1589.
 - 26 Cahill DP, Lengauer C, Yu J, Riggins GJ, Willson JK, Markowitz SD, et al. Mutations of mitotic checkpoint genes in human cancers. *Nature*. 1998;392:300–303.
 - 27 Yamada HY, Gorbsky GJ. Spindle checkpoint function and cellular sensitivity to antimitotic drugs. *Mol Cancer Ther*. 2006;5:2963–2969.
 - 28 Niikura Y, Dixit A, Scott R, Perkins G, Kitagawa K. BUB1 mediation of caspase-independent mitotic death determines cell fate. *J Cell Biol*. 2007;178:283–296.
 - 29 Castedo M, Perfettini JL, Roumier T, Andreau K, Medema R, Kroemer G. Cell death by mitotic catastrophe: a molecular definition. *Oncogene*. 2004;23:2825–2837.
 - 30 Ha GH, Kim HS, Lee CG, Park HY, Kim EJ, Shin HJ, et al. Mitotic catastrophe is the predominant response to histone acetyltransferase depletion. *Cell Death Differ*. 2009;16:483–497.
 - 31 Beyer CF, Zhang N, Hernandez R, Vitale D, Nguyen T, Ayral-Kaloustian S, et al. The microtubule-active antitumor compound TTI-237 has both paclitaxel-like and vincristine-like properties. *Cancer Chemother Pharmacol*. 2009;64:681–689.
 - 32 Iuchi K, Akagi K, Yagura T. Heterocyclic organobismuth(III) compound targets tubulin to induce G2/M arrest in HeLa cells. *J Pharmacol Sci*. 2009;109:573–582.
 - 33 Pathan N, Aime-Sempe C, Kitada S, Basu A, Haldar S, Reed JC. Microtubule targeting drugs induce bcl-2 phosphorylation and association with Pin1. *Neoplasia*. 2001;3:550–559.
 - 34 Gascoigne KE, Taylor SS. Cancer cells display profound intra- and interline variation following prolonged exposure to antimitotic drugs. *Cancer Cell*. 2008;14:111–122.
 - 35 Blagosklonny MV. Prolonged mitosis versus tetraploid checkpoint: how p53 measures the duration of mitosis. *Cell Cycle*. 2006;5:971–975.
 - 36 Karna P, Sharp SM, Yates C, Prakash S, Aneja R. EM011 activates a survivin-dependent apoptotic program in human non-small cell lung cancer cells. *Mol Cancer*. 2009;8:93.
 - 37 Pourroy B, Carré M, Honoré S, Bourgarel-Rey V, Kruczyński A, Briand C, et al. Low concentrations of vinflunine induce apoptosis in human SK-N-SH neuroblastoma cells through a postmitotic G₁ arrest and a mitochondrial pathway. *Mol Pharmacol*. 2004;66:580–591.
 - 38 Mansilla S, Priebe W, Portugal J. Mitotic catastrophe results in cell death by caspase-dependent and caspase-independent mechanisms. *Cell Cycle*. 2006;5:53–60.
 - 39 Hsu SL, Yu CT, Yin SC, Tang MJ, Tien AC, Wu YM, et al. Caspase 3, periodically expressed and activated at G2/M transition, is required for nocodazole-induced mitotic checkpoint. *Apoptosis*. 2006;11:765–771.
 - 40 Beswick RW, Ambrose HE, Wagner SD. Nocodazole, a microtubule depolymerising agent, induces apoptosis of chronic lymphocytic leukaemia cells associated with changes in Bcl-2 phosphorylation and expression. *Leuk Res*. 2006;30:427–436.
 - 41 Kim M, Murphy K, Liu F, Parker SE, Dowling ML, Baff W, et al. Caspase-mediated specific cleavage of BubR1 is a determinant of mitotic progression. *Mol Cell Biol*. 2005;25:9232–9248.
 - 42 Perera D, Freire R. Human spindle checkpoint kinase Bub1 is cleaved during apoptosis. *Cell Death Differ*. 2005;12:827–830.
 - 43 Kagawa S, Gu J, Honda T, McDonnell TJ, Swisher SG, Roth JA, et al. Deficiency of caspase-3 in MCF7 cells blocks Bax-mediated nuclear fragmentation but not cell death. *Clin Cancer Res*. 2001;7:1474–1480.